A Planar Conformal Microwave Resonator for Subcutaneous Imaging

Sen Bing and J.-C. Chiao

Southern Methodist University, Dallas, TX, USA (sbing@smu.edu)

Abstract— A planar conformal microwave resonator is developed to detect malignant tumors inside tissues. The tuned sensor with localized field distributions can noninvasively distinguish permittivity variations within tissues. The principle is based on electromagnetic-wave interaction in materials where permittivity variations due to malignant tumors among normal tissues affect the field distributions. The imaging process is conducted with a two-dimensional raster scan to record reflection coefficients in pixels. The normalized resonant frequencies and magnitudes of reflection coefficients are fused to generate localization maps. The concept is validated by promising results with tumor phantoms at different depths and of various sizes. The fused maps indicate a great potential for subcutaneous imaging on the skin in a more efficient and safer way with lower costs than the traditional nondestructive evaluation methods such as X-ray.

I. INTRODUCTION

Currently, X-ray mammography is the primary breast tumor screening and diagnosis method [1], but it has been limited by its high cost, discomfort, and high recall rates, requiring additional imaging and biopsy [2, 3]. Frequent X-ray exposure may lead to potential risks to human health. Magnetic resonance imaging (MRI) has been used to increase screening accuracy. However, its instrument costs and operation requirements are higher than mammography, further increasing patients' stress and financial burden. Such inconvenience adds behavioral delay for routine check-ups in the potential cancer patient population. These factors call for a new sensing modality that is convenient, affordable, and safe, serving as a quick first-step screening tool. Radio-frequency and microwave sensing has been investigated, providing benefits of nonionizing radiation [4]. Conventional methods utilize wave propagation and scattering based on radar principles to detect tumors [5]. Instrumentation with multiple antennas and algorithms for beamforming and time delays may add costs and operational complexity. This work aims to develop a compact and planar imaging system with a microwave resonator on a flexible polymer substrate that can locate subcutaneous tissue abnormalities.

II. RASTER SCAN WITH THE RESONATOR

We have developed a self-tuned method for impedance matching in planar loop resonators by embedding a metal pad as the tuning element [6]. The metal pad provides distributed reactances that can be used to match impedance at a desired operating frequency, achieving a high-quality factor. The tuned loop structure is highly susceptible to permittivity variations with localized electric fields in the tissues [7]. Based on the principle, it can be used to sense malignant tumors among

normal tissues, where the boundaries of permittivities cause inconsistency in the interaction of electromagnetic fields.

The resonator is designed on a flexible substrate with a thickness of 76 µm. The loop has a radius of 5.7 mm with a metal width w of 0.7 mm and a center metal pad, as shown in Fig. 1. The spacing gap between the loop and pad is tuned as 1.95 mm to obtain a quality factor of 173.1 at 2.423 GHz. Without the tuning pad, the quality factor is only 2.8. In finiteelement simulations, the phantom includes three parts: the skin with a 2-mm thickness, normal breast tissues, and a malignant tumor of 17.1×17.1×17.1 mm³. Measurements with the same physical constructions to validate the simulation models have been conducted [8]. Dielectric constants utilized for breast skin, breast tissues, and tumors are 38, 6, and 59, while the corresponding conductivities are 1.45, 0.13, and 2.8 S/m, respectively [9–11]. The loop is tuned at the ISM (Industrial, Scientific, and Medical) band frequency of 2.45 GHz. When the malignant tumor is directly underneath the loop at a depth of 8 mm, the resonant frequency shifts from 2.423 to 2.341 GHz, while the magnitude of the reflection coefficient changes from -68.8 to -33.8 dB.

The process of tumor localization can be realized by a 2-dimensional discrete raster scan with the sensor moving across the skin surface. Based on the reflection coefficients, heatmaps are generated from resonant frequencies and reflection coefficients, as shown in Figs. 2(a) and (b), respectively. Each pixel is set at 17.1² mm², and both maps can identify the tumor location. In Fig. 2(a), the contrasts from the tumor pixel to the neighboring pixels are 92, 102, 98, and 81 MHz. The magnitude contrasts are 13.6, 21.3, 38.6, and 10.1 dB in Fig. 2(b).

Although the contrasts are obvious to identify the tumor location in Fig. 2(a) for human eyes, in some cases the resonant



Figure 1. The microwave resonator on a flexible substrate.

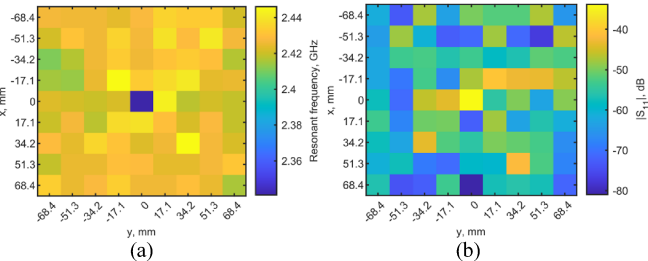


Figure 2. Maps generated from reflection coefficients for a tumor at a depth of 8 mm. The tumor is located at (x=0,y=0). (a) Map of resonant frequencies. The dark blue color pixel indicates the tumor location. (b) Map of $|s_{11}|$. The 335 light yellow color pixel indicates the tumor location.

frequencies do not monotonically shift when the tumor location changes depth. The heatmaps then become noisy. This is due to the non-uniform and anisotropic field distributions in the tissues affecting the contribution of tumor permittivity to the effective permittivity experienced by the sensor. Different from our previous results that only utilized frequency shift data [8], the magnitudes of reflection coefficients can also be used to reconstruct heatmaps. The resonant frequencies and reflection coefficient magnitudes at each pixel are first normalized to their ranges between the minimum and maximum values. Two maps with scales from zero to one are generated. A weighting factor is selected to fuse these two heatmaps together to achieve a better contrast on the boundaries of pixels in order to identify the tumor location.

Figure 3 shows the fused image with a weighting factor of 0.5 (meaning equal weights between two normalized maps), which is selected for illustration purpose. The implant location is clearly indicated with the dark pixel. The fused scales are zero at the center, and 0.84, 0.95, 0.97, and 0.74 at the neighboring pixels, showing high contrasts. The weighting factor can be chosen from 0.01 to 0.99 to construct the map with the highest contrast. Furthermore, scans with smaller pixel sizes

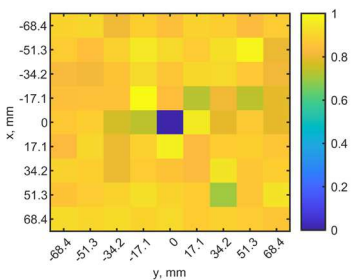


Figure 3. Fused map from the normalized resonant frequency and $|s_{11}|$ maps. The tumor is located at (0,0) with a depth of 8 mm.

can increase spatial resolutions by oversampling.

III. DETECTION SENSITIVITY

To investigate detection sensitivity, simulations are conducted with smaller tumors with a cubic length from 6 to 17.1 mm and at a depth range from 5 to 40 mm. Reflection coefficients are recorded with the sensor above the tumor at (0, 0) and its adjacent pixel (0, 17.1). Normalized resonant frequencies and $|s_{11}|$ at (0, 0) with respect to those at (0, 17.1) are shown in Figs. 4(a) and (b). The trends in resonant frequency shifts show the limit of detection at about 15 mm, while with the normalized $|s_{11}|$ at 20 mm for different sizes of tumors. The trends do not monotonically change with tumor depth or size.

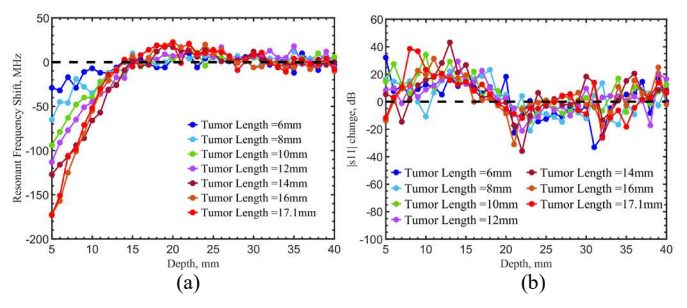


Figure 4. (a) Resonant frequency shifts and (b) changes of $|s_{11}|$ between pixels (0, 0) and (0, 17.1) with different tumor sizes at varied depths to test the detection sensitivities.

Again, it is because the electrical field distributions in the tissues affect the effective permittivities. A tumor with longer lengths than 8 mm can be recognized up to a depth of 20 mm, and 15 mm for 6- and 8-mm sizes. The contrasts are only compared between two pixels in Fig. 4. The construction of 2-D fused images with the normalized parameters among pixels and optimized weighting factors can further enhance the visibility of tumor boundaries. Further investigations with oversampling and beam-forming techniques are in progress to enhance the spatial resolutions at deeper tissues.

IV. CONCLUSION

We have investigated the ability of a resonant loop that conforms to the skin to detect tissues' effective permittivity variations in space. Electromagnetic fields are altered in the presence of a tumor and the high-quality factor resonance can sense the irregularity with a sufficient spatial resolution. A construction method of fused images from the maps of normalized resonant frequencies and magnitude of reflection coefficients is demonstrated. The proposed nondestructive evaluation method to identify tissue abnormality in this work is safer without ionizing effects, and more convenient and efficient as the instrument is directly placed and confirmed on the skin. It can be applied as the first-step tumor-screening modality before conventional methods to increase accuracy.

ACKNOWLEDGMENT

The authors sincerely appreciate the support of the National Science Foundation grant ENG-CMMI-1929953 and the Mary and Richard Templeton endowment.

REFERENCES

- [1] E.C. Fear, "Microwave Imaging of the Breast," *Technology in Cancer Research & Treatment*, vol. 4, pp. 69-82, Feb. 2005.
- [2] P.T. Huynh, A.M. Jarolimek and S. Daye, "The false-negative mammogram," *Radiographics*, vol. 18, pp. 1137-1154, 1998.
- [3] S.W. Fletcher and J.G. Elmore, "Mammographic Screening for Breast Cancer," *New Eng J. of Med.*, vol. 348, pp. 1672-1680, 2003.
- [4] H. Omer, "Radiobiological effects and medical applications of non-ionizing radiation," *Saudi J. Biol. Sci*, vol. 28, pp. 5585-5592, 2021.
- [5] J.-C. Chiao, et al. "Applications of Microwaves in Medicine," IEEE Journal of Microwaves, vol. 3, pp. 134-169, 2023.
- [6] S. Bing, K. Chawang and J.-C. Chiao, "A Self-Tuned Method for Impedance-Matching of Planar-Loop Resonators in Conformable Wearables," *Electronics (Basel)*, vol. 11, pp. 2784, 2022.
- [7] S. Bing, K. Chawang and J.-C. Chiao, "A Resonant Coupler for Subcutaneous Implant," Sensors (Basel), vol. 21, pp. 8141, 2021.
- [8] S. Bing, K. Chawang and J.-C. Chiao, "A Flexible Tuned Radio-Frequency Planar Resonant Loop for Noninvasive Hydration Sensing," IEEE Journal of Microwaves, pp. 1-12, 2022.
- [9] S. Gabriel, R.W. Lau and C. Gabriel, "The dielectric properties of biological tissues: II. Measurements in the frequency range 10 Hz to 20 GHz," *Phy. in Med. & Biology*, vol. 41, pp. 2251-2269, 1996.
- [10] T. Sugitani, et al. "Complex permittivities of breast tumor tissues obtained from cancer surgeries," App. Phy. Let., vol. 104, 253702, 2014.
- [11] M. Lazebnik, et al."A large-scale study of the ultrawideband microwave dielectric properties of normal breast tissue obtained from reduction surgeries," Phy. in Med. & Biology, vol. 52, pp. 2637-2656, 2007.